doi.org/10.36721/PJPS.2021.34.5.SUP.1849-1859.1

Preparation of smart PVP/HPMC based IPN hydrogel, its characterization and toxicity evaluation

Hammad Yousaf[1], Ikrima Khalid[1]*, Kashif Barkat[2], Ikram Ullah Khan[1] and Yasir Mehmood[3,4]

[1]Department of Pharmaceutics, Faculty of Pharmaceutical Sciences, Government College University Faisalabad, Pakistan
[2]Faculty of Pharmacy, University of Lahore, Lahore Pakistan
[3]Ameer & Adnan Pharmaceuticals, Lahore, Pakistan
[4]Rashid Latif College of Pharmacy, Lahore, Pakistan

Abstract: In this study, the interpenetrating polymeric network (IPN) were fabricated via free radical polymerization using polymers hydroxypropyl methylcellulose (HPMC), Polyvinylpyrrolidone (PVP) and monomer Methacrylic acid (MAA) and also investigated their influence by changing their concentrations. The developed polymeric network is crosslinked via N′ N' -methylene bis-acrylamide (MBA). Different characterizations have been performed to analyze fabricated interpenetrating polymeric network structure i.e., Scanning Electron Microscopy (SEM), X-ray Powder Diffraction (XRD), Fourier-Transform Infrared Spectroscopy (FT-IR), Thermo-gravimetric Analysis (TGA) and Differential Scanning Calorimetry (DSC). Letrozole (LTZ) was loaded as a model drug in the developed system. Swelling dynamics as well as drug release behavior were thoroughly examined. FTIR studies corroborated the formation of interpenetrating polymeric network. SEM uncovered porous structure while TGA depicted enhanced thermal stability of polymeric network. PXRD depicted amorphous dispersion of LTZ. Swelling dynamics as well as LTZ release behavior from developed interpenetrating polymeric network hydrogels were dependent upon pH of the medium and concentration of pure reactants employed. Higuchi model was best fit to regression coefficient which indicated diffusion controlled mechanism of drug release. Acute oral toxicity study depicted no mortality or any signs relating to acute toxicity throughout the whole observed period. Hence, the designed interpenetrating polymeric network might turn out to be a safe and a potential carrier system for the delivery of LTZ in the treatment of breast cancer (BC).

Keywords: IPN, Hydrogel, Letrozole, HPMC, PVP, MAA, pH- sensitive, breast cancer.

INTRODUCTION

Basic purpose of formulating novel drug delivery system (NDDS) is to eliminate barriers of conventional active ingredient delivery system Saraf (2010). Control drug delivery system (CDDS) releases drug at particular rate for specific period of time maintaining constant concentration of active moiety at targeted site (Ganji and VASHEGHANI, 2009). Variations in plasma drug level and patient non-compliance were the limitations which have led the transition from conventional dosage from towards CDDS (Khalid *et al*., 2018).

Over the past few years, the pharmaceutical industry has eyed upon polymer as well as material science, ensuing evolving evolution of NDDS. A vast variety of NDDS such as liposomes, vesicles, polymers, implants, micelles, nanoparticles, 3 dimensional polymeric network, microspheres, etc., was thoroughly exploited and depicted various advantages. By using NDDS Active ingredient solubility, stability, bioavailability, pharmacological activity, can be enhanced and they also provide protection against toxicity, physical and chemical degradation and sustained active ingredient release. Along with a few limitations like delayed onset and increased potential of first pass effect (Khalid *et al*., 2018), (Bhowmik *et al*., 2012). In this regard, hydrogels are most promising drug delivery system to achieve controlled drug delivery.

Hydrogels are also known as hydrophilic gels because they possess attributes of both solid and liquid. They have a three dimensional polymeric network system which is capable of absorbing great amount of water, making them very hydrophilic in nature but still they remain un-dissolved in water. Water imbibition tendency of hydrogels depends upon polymeric network constitutional factors and swelling medium (Sami *et al*., 2018). Among various types of polymeric networks, interpenetrating polymeric system (IPN) are becoming more important (Ahmed, 2015), (Soman *et al*., 2014).

Polymer blends prove to be the answer for the conception of new materials, depicting suitable flexibility for the readjustment of the drug release. In present research, polymer blends consisting of polyvinylpyrrolidone (PVP) and hydroxypropyl-methylcellulose (HPMC) have been thoroughly studied with an aim to design an adjustable system. PVP is a water-soluble polar tertiary amide as well as a potent Levis base. Fabrication of hydrogel using PVP is also reported by Anwar *et al*. (2021). HPMC is a sparingly water-soluble polar polymer and swell when

*Corresponding author: e-mail: ikrima_khalid@yahoo.com

come in contact with solution, resulting into gel mass. Khanum *et al*. (2018) successfully prepared pH sensitive HPMC based hydrogels *via* free radical polymerization previously.

Letrozole (LTZ) is a selective anticancer drug employed in the prophylaxis and treatment of breast cancer (BC). LTZ, a non-steroidal competitive blocker of the aromatase enzyme system; blocks the changeover of androgens into estrogens. LTZ is rapidly and completely absorbed from the gastrointestinal tract (Group, 2005). LTZ is associated with side effects like hot flashes, mild to moderate hair loss, arthralgia-like joints, muscles and bone pain, tiredness, fatigue, unusual sweating, nausea, dizziness, trouble sleeping, diarrhoea, drowsiness, weight gain, constipation, headache, numbness, tingling, weakness, stiffness in hand and fingers (Khan *et al*., 2010). Up till today, very scarce studies have been conducted on developing a CDDS in order to scale down LTZ adverse effect profile (Siddiqa *et al*., 2014) like Kazemi *et al*. (2016) synthesized and evaluated a controlled drug delivery system based on the magnetic molecularly imprinted nanoparticles for the LTZ to decrease the adverse effects of LTZ and Radwan *et al*. (2021) incorporating LTZ into PLGA nanoparticles in order to improve its therapeutic efficacy, control the drug release, and minimize side effects. To the best of our knowledge no research study is known to be reported on hydrogel for this anticancer drug.

In this study, we fabricated and examined CDDS based upon the IPN hydrogel for the delivery of LTZ. IPN hydrogel was characterized via FTIR, PXRD, TGA, DSC and SEM. Several experiments have been conducted to examine the recognition characteristics of developed IPN hydrogels. Swelling and active ingredient release studies were conducted to examine fabricated IPN hydrogel for LTZ delivery. *Ex-vivo* toxicity study has also been carried out on animal models to evaluate toxicity of prepared formulation.

MATERIALS AND METHODS

Materials

Letrozole (99.8%) (Mfg. date: 10-01-2019, Exp. Date: 09-01-2022) was incurred from a pharmaceutical company as gift sample.Pure polymers hydroxypropyl methylcellulose (HPMC-K15) and Polyvinylpyrrolidone (PVP K30) were bought from Sigma-Aldrich (Gillingham, UK). Monomer Methacrylic acid (MAA) and cross linker MBA were also obtained from Sigma-Aldrich (St. Louis, USA). Initiator ammonium per-sulfate (APS) was supplied by Fluka-Amtsgericht Stuttgart, Denmark.

Synthesis

Free radical solution polymerization technique has been used for preparing the pH sensitive controlled release IPN hydrogels of LTZ (Akhtar *et al*., 2016). Weighed amount of polymers (HPMC and PVP) were dissolved in water separately and then mixed at constant temperature until a transparent solution (A) was obtained. Nitrogen stream employed to evacuate the entangled oxygen. Solutions of initiator (APS) and monomer (MAA) were prepared by dissolving them in water separately and then mixed to get solution (B). Solutions (B) was gradually poured in solution (A) drop by drop with constant stirring. At last, cross-linker (MBA) of weighed quantity was incorporated into the reaction mixture. The temperature was raised in a gradual manner so as to avert auto acceleration as well as production of bubbles. Temp scheme for polymerization of liquid mixture has been kept at $45^{\circ C}$ up to 1 hour, $50^{\circ C}$ up to 2 hours, $55^{\circ C}$ up to 3 hours, $60^{\circ C}$ up to 4 hours, as well as $65^{\circ C}$ up to 24 hours. Following this period, obtained cylindrical gel was cut unto discs of sizes ranging from 6mm to 8mm. To remove the unreacted materials, discs were placed in 50% (v/v) ethanol. The discs were then carefully dried firstly at $25^{\circ C}$. Than oven drying at 40-$45^{\circ C}$ till the solid attained constant mass. fig. 1 depicts possible cross linked polymeric structure.

Characterization

Fourier-Transform-Infrared-Spectroscopy (FTIR)

For measuring and recording spectra of reactants as well as LTZ loaded hydrogels, IPN hydrogels were subjected to crushing to incur desired size. A value ranging between 4000 to 600cm^{-1} has been chosen for spectral scans through the employment of Bruker FTIR (Tensor 27 Series - Bruker Corporation - Germany) instrument, employing attenuated-total-reflectance (ATR) technology that was accompanied by software OPUS data collection (Kamoun, 2016, Acharjya *et al*., 2010).

Thermal Analysis

TGA of the polymers, formulation sample and monomer has been carried out on thermal analysis system (TA instrument Q2000 Series - West Sussex - UK). For TGA, sufficient heating of samples at 10◦C per minute up till 500◦C was conducted within a N2 atmosphere (Rusu *et al*., 2015).

Powder X-Ray Diffraction (PXRD)

IPN hydrogels nature was examined through PXRD. The specimens were examined employing X-ray diffractometer (x-Pert- PAN analytical- The Netherlands). Diffraction angle ranges from 10 to 50◦.

Scanning Electron Microscopy (SEM)

Surface morphology of IPN polymeric network has been examined via employing SEM. Hydrogel sample was placed on mount made up of aluminium mount and sputtered through gold palladium. 20 KV accelerated voltage, comprising 5-15mm space distance, has been employed for scanning samples (Dutta *et al*., 2016).

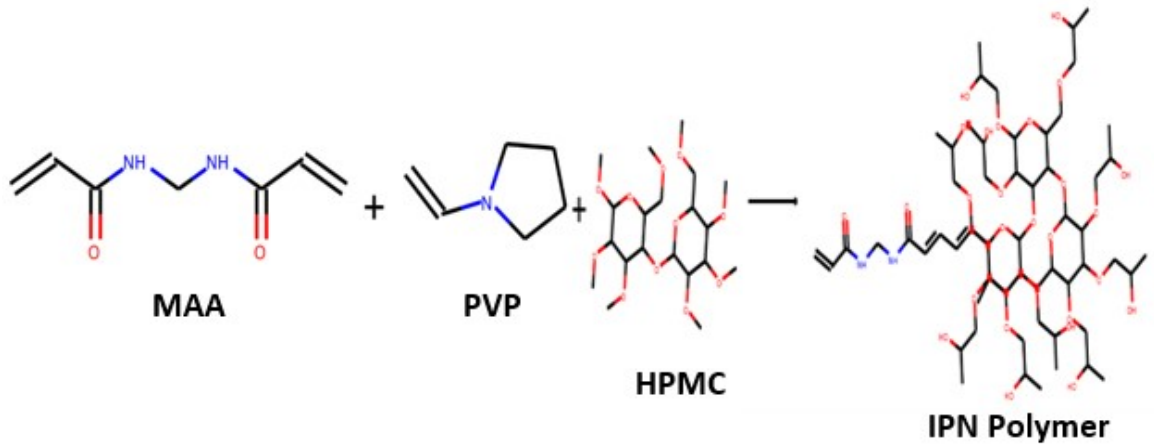

Fig. 1: Chemical reaction involving synthesis of IPN hydrogel

Code	Polymers		Monomer	Cross-linker	Initiator
	PVP g/100g	HPMC g/100g	MAA g/100g	MBA mol%	APS g/100g
F_1	0.8	0.4	24	0.032	0.32
F_2	1.6	0.4	24	0.032	0.32
F_3	2.4	0.4	24	0.032	0.32
F_4	1.6	0.4	24	0.032	0.32
F_5	1.6	0.8	24	0.032	0.32
F_6	1.6	1.2	24	0.032	0.32
F_7	1.6	0.4	16	0.032	0.32
F_8	1.6	0.4	24	0.032	0.32
F_9	1.6	0.4	32	0.032	0.32

Gel%, yield% and gel time

gel% and yield% was selected to estimate how much quantity of reactant polymerized in formulating hydrogels. Firstly within vacuum oven hydrogels were dried till constant weight (m_i) and afterwards the polymeric network were sufficiently macerated within H2O for a period of 7 days along with periodic agitation and shaking to discard if any polar portion. Within oven water immiscible portion of polymeric network was subsequently dried to achieve a constant-weight (m_d) Gel and yield% have been acquired by

$$Gel\% = \frac{m_d}{m_i} \times 100$$

$$Yield\% = \frac{m_d}{m_c} \times 100$$

Where m_c is weight in totality of reactants of developed formulation. (Fu and Soboyejo, 2010)

Swelling study

pH sensitive behaviour of IPN hydrogels has been evaluated by performing dynamic swelling studies at pH 1.2 utilizing 0.1M HCl at pH 7.4 utilizing 0.2 M phosphate buffer solution at temperature 37°C. After weighing, the dried polymeric discs were put in swelling media with occasional withdrawal and weighing till uniform weight of hydrogel was acheived. Normalized-swelling-degree Q at time t was computed in grams of water per gram of dry gel utilizing the succeeding expression:(Ahmadi *et al*., 2015).

$$Q_t = \frac{m_t - m_o}{m_o}$$

m_t = IPN hydrogel weight after swelling.
m_o = IPN Hydrogel weight before swelling (dry gel).
Q_t = weight of water absorbed
Normalized equilibrium swelling Q_∞ is estimated through

$$Q_\infty = \frac{m_t - m_o}{m_o}$$

Loading of Letrozole

The LTZ loading was performed through plunging IPN polymeric network in solution of LTZ 1% w/v ethanol-water (50:50% v/v) mixture up-to 7 days. The swelled hydrogels were brought out from the mixture, dried at room temperature with further drying in oven until constant weight was attained (Sohail *et al*., 2015).

Determination of Drug Entrapment Efficiency (DEE)

To determine DEE, LTZ loaded hydrogels was crushed within mortar and pestle of known weights. Then dipped in phosphate buffer (25ml, pH 7.4) for duration of 24 hour. To extract LTZ sonication was performed for duration of 20. Analysis of clear supernatant solution was performed for LTZ via UV-Visible Spectrophotometer at λ max (240 nm) (Barkat *et al*., 2017). Through following equation entrapment efficiency of formulated hydrogels for LTZ has been estimated (Anwar *et al*., 2020).

$$\% \text{ Entrapment efficiency} = \frac{\text{Actual drug content in IPN hydrogel}}{\text{Theoretical drug content in IPN hydrogel}} \times 100$$

Release study

USP Dissolution Apparatus has been utilized to measure drug release at acidic pH 1.2 and basic pH 7.4. The weighed polymer disc was placed in dissolution medium of 900ml and stirred at 50rpm to maintain a uniform drug concentration with in the dissolution medium. The temperature of the dissolution medium was controlled at 37^{o}C.Samples were collected after specific time intervals up to 36 hrs. Every time fresh medium was used to replace sampled volume. LTZ release was determined at λ_{max} 240 nm. (Malik *et al*., 2017).

Analysis of drug release kinetics

Krsmeyer-Peppas (Chavda and Patel, 2010), Higuchi (Kim *et al*., 1992), first order (Singh and Sharma, 2014), zero order (Varelas *et al*., 1995) were used to appropriately find out the drug release rate and mechanism.

Oral Acute Toxicity Study

Based on maximum DEE as well as *in-vitro* cumulative LTZ release, (F6) polymeric formulation was selected to evaluate safety through toxicity study. The toxicity evaluation has been affirmed in accordance with Organization for Economic Co-operation and Development (OECD) authentic guidelines. 10 healthy adult albino rabbits (Purchased from Animal Facility Center of University of Veterinary and Animal Sciences (UVAS), Lahore, Pakistan) of weights ranging from approximately 2.0 to 2.5kg have been utilized for conducting this study. Separated with in 2 groups, every group has 5 numbers of rabbits. Maximum tolerance dose (MTD) method was selected to evaluate toxicity. Animals transitory room (with room temperature ranging from 25 ±2◦C and relative humidity ranging from 65±5%, along with 12 hour light-dark cycle) was utilized for housing of all animals. Each rabbit had been sustained through water ad libitum along with a balanced dietary sustenance. Regular monitoring of rabbits for general conditions and well-being was undertaken (such as energy, activity, hair, behavior, feces, along with a few clinical signs), variation in mortality, body weight, as well as morbidity. Hence, fourteen days later, rabbits had been subjected to sacrificial cervical dislocation. All the vital organs (such as spleen, heart, kidney, liver, lungs and stomach) had been dissected and weighed appropriately. All the organs had been conserved in buffered- formaldehyde (10%), imbedded within paraffin, following segmentation. Haematoxylin-eosin was selected to stain paraffin section to conduct histopathological examination.

Ethical approval

This animal research study conducted had been reviewed and approved through careful assessment and consideration of Pharmacy Research Ethics Committee (PREC) of GCUF, Faisalabad, Pakistan.

STATISTICAL ANALYSIS

All experimental data was expressed as mean ± standard deviation (SD) and calculated by Microsoft Excel 2013 and Origin Pro version 8.5.1.

RESULTS

FT-IR [Fourier Transform Infra-Red spectroscopy]

To affirm the chemical structures of the synthesized IPN hydrogels, the FTIR spectroscopy was conducted. FTIR spectra of HPMC, PVP, MAA and developed unloaded IPN hydrogel have been shown in fig. 2.

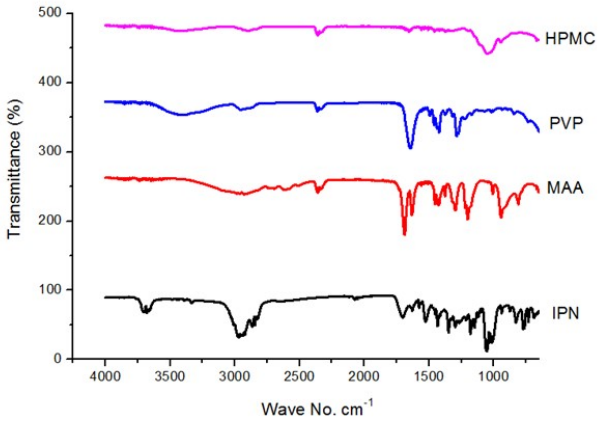

Fig. 2: FTIR Spectra depiction of (HPMC), (PVP), (MAA) and (IPN Hydrogel).

Scanning Electron Microscopy (SEM)

When SEM was performed on formulated IPN polymeric formulation it depicts porous structure as in fig. 3.

Thermal Analysis

Fig. 4 depicts TGA of LTZ, formulated IPN hydrogel (unloaded and LTZ loaded). No remarkable weight change (about 8%) observed in unloaded IPN up to 160°C. However, from 160°C to 200°C it showed max weight loss i.e.; 20% which lead to degradation upon increasing further temperature. TGA thermogram of LTZ showed weight loss in different stages. During first stage, it showed 5 % weight loss up to 90°C which may be due to water loss. During the second stage (90°C to 180°C), it showed high weight loss of 55% which correspondence the partial degradation of LTZ. During last stage from 180°C to 240°C, it showed complete degradation.

TGA thermogram of loaded IPN also showed three stages weight loss. Initial weight loss is up to 180°C (20% weight lose) which indicated the degradation half-life of LTZ in IPN hydrogel is better than LTZ alone and IPN corresponding toward more stability. The second stage weight loss of IPN is about 55% (180°C to 210°C) which

is due to polymer breakdown at high temperature. Further rise in temperature resulted in complete degradation of IPN hydrogel. From results, we concluded that LTZ loaded IPN is more stable than alone LTZ (Khalid *et al*., 2018).

Due to volatile compounds DSC thermogram of LTZ demonstrate endothermic peak at 40°C -98°C owing towards dehydration and elimination of other volatile components. Due to LTZ degradation, peak was observed around 210°C. The glass transition temperature Tg of the LTZ, loaded and unloaded IPN hydrogel is 50°C.

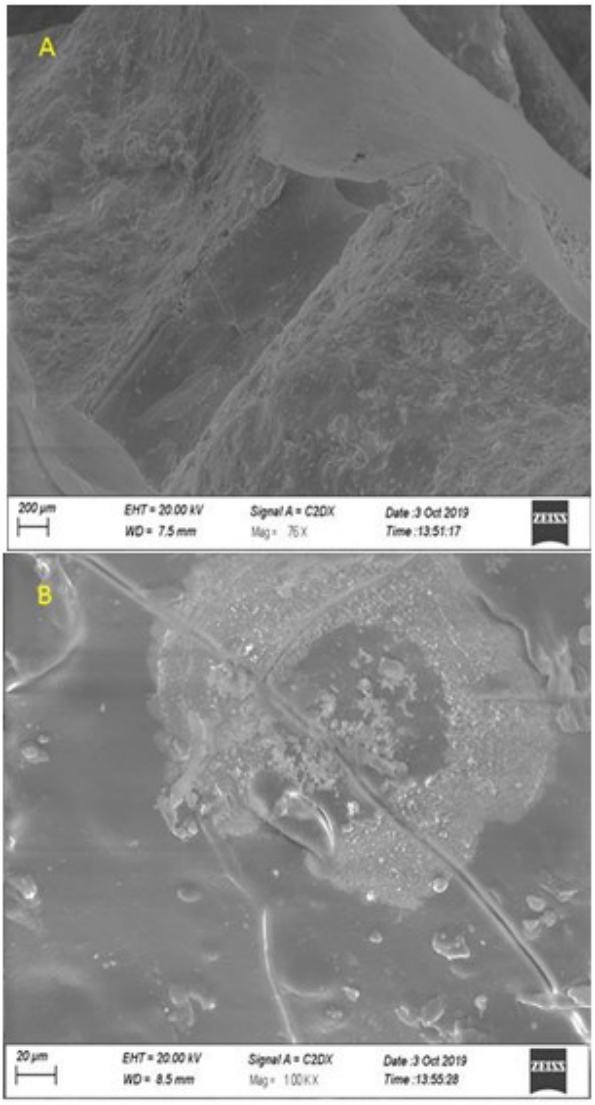

Fig. 3: SEM image depiction of IPN hydrogel at different magnifications

Powder X-Ray Diffraction (PXRD) Analysis

PXRD spectrum of LTZ, unloaded IPN hydrogel and loaded IPN hydrogel have been shown in fig. 6 with the intention to study the physical behaviour of the LTZ in hydrogel. The sharp, shrill as well as intense peaks at 2θ = 07.2°, 11.12°, 14.16°, 16.24°, 20.16°, 21°, 21.44°, 23°, 24.16°, 25.08°, 26.52°, 28.8°, 33.6°, 35° and 39° are a characteristic feature of LTZ depicting majorly a crystalline nature of drug. The number of peaks affirms the various crystalline forms that are present in LTZ. Due to reduced crystallinity PXRD analysis of unloaded hydrogel showed opaque peaks because of monomer conjugation MAA with polymers (HPMC & PVP) using MBA (cross linker) which leads to enhancement in amorphous phase fraction. PXRD of LTZ filled hydrogel, the shrill and sharp, as well as features of characteristic peaks of LTZ had been interchanged by dense peaks, depicting a reduction in crystallinity, whereas the presence of typical peaks of LTZ depicts LTZ crystalline nature within loaded hydrogel stays the same.

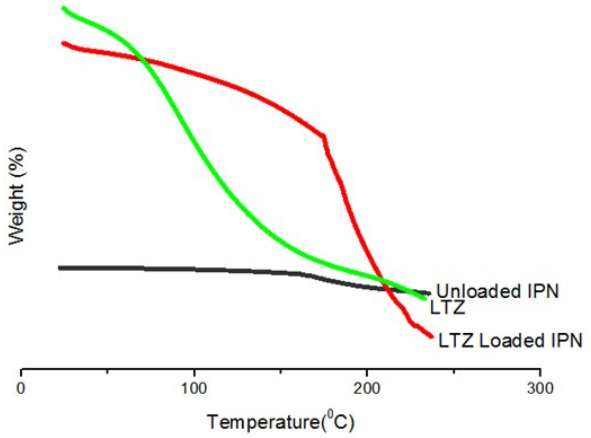

Fig. 4: TGA of Letrozole (LTZ), Loaded IPN and unloaded IPN

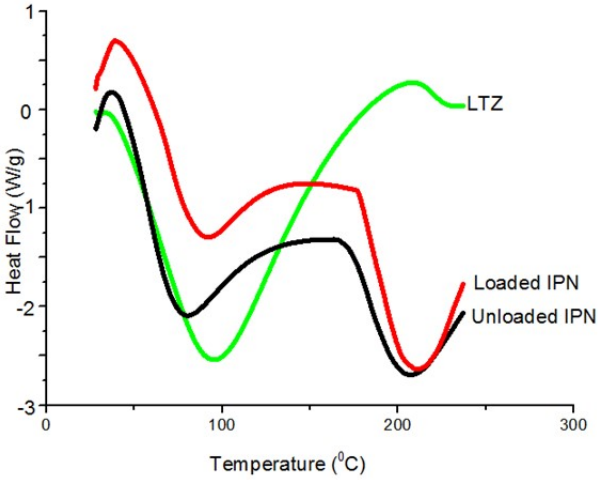

Fig. 5: DSC of Letrozole (LTZ), Loaded IPN and unloaded IPN

Gel time, Gel% and Yield%,

The gel time, gel% and yield% findings have been shown in fig. 7. Direct relation exists between MAA quantity and gel %, yield % whereas Gel time decreased with increased concentration of MAA shown in fig. 7a. PVP

concentration showed inverse relation to the yield % and gel time whereas gel % is not effect by PVP concentration. The fig. 7 C described that increasing HPMC concentration caused increase in yield % and gel time whereas gradual decrease can be seen in gel %.

Swelling Study

Imbibition studies were performed at different pH solutions, their results are shown in fig 8. Like other anionic hydrogels, the IPN hydrogel exhibits a pH-dependent expansion behavior. High swelling ratio has been seen at pH 7.4.

Drug entrapment efficiency and release study

The drug entrapment successfully done in the hydrogels, as shown in table 1. The drug entrapment of the hydrogels was directly related to the water uptake of the polymeric network system. Drug loading was also dependent on the pH environment of the media, and greater drug entrapment was observed at higher pH.

In vitro drug release behavior under physiological conditions has been examined to evaluate the probable application. The cumulative percentage of drug released from polymeric carriers at pH 1.2 and 7.4 as a function of time has been depicted in fig. 10.

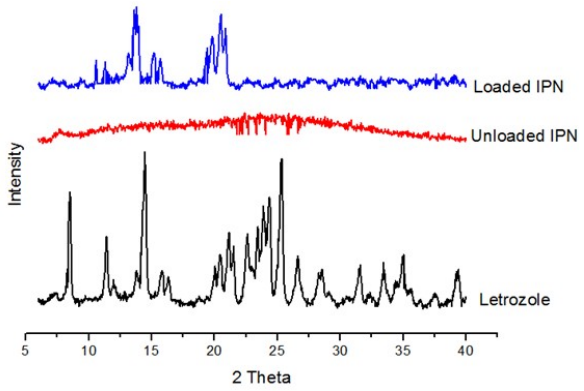

Fig. 6: XRD of Letrozole (LTZ) and prepared IPN Unloaded and Loaded

Table 1: Drug entrapment efficiency (%DEE) & percent drug release on pH 1.2 and pH 7.4.

Code	Drug Entrapment Efficiency	Percent release of LTZ (for a 24 hour period)	
		pH 1.2	pH 7.4
F_1	51.32	8.9	81.23
F_2	62.30	9.1	82.93
F_3	63.14	9.3	83.13
F_4	62.30	9.1	82.93
F_5	64.32	10.2	80.40
F_6	69.24	9.9	87.43
F_7	62.30	9.1	82.93
F_8	58.39	10.3	81.53
F_9	59.34	9.6	75.93

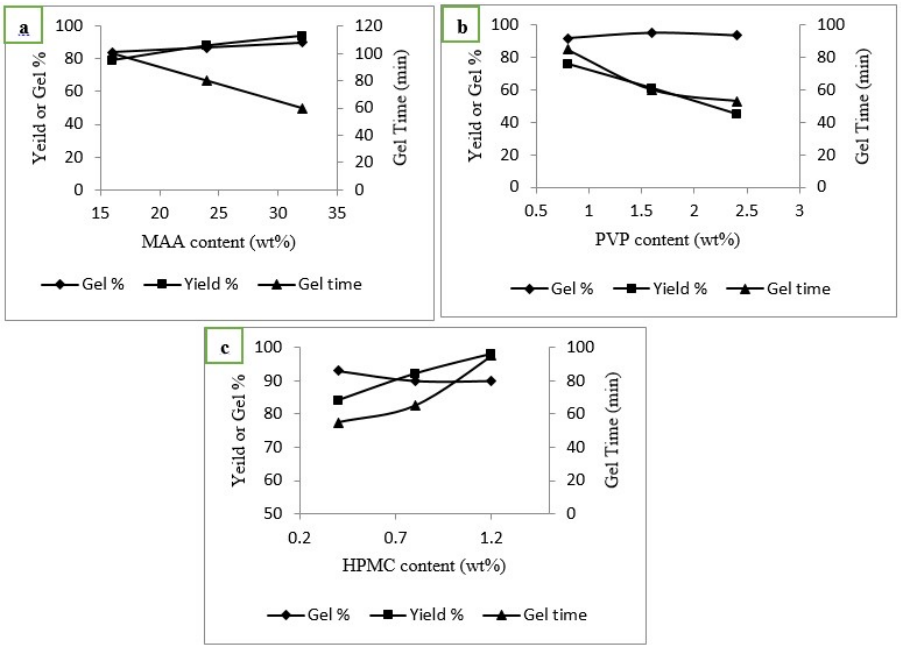

Fig. 7: Effect of (a) MAA; (b) PVP; (c) HPMC on gel%, yield% and gel time.

Table 2: Drug Release Kinetics of each and every HPMC-PVP-MAA polymer formulation

Sample name	Dissolution Media	Zero Order Kinetics		First Order Kinetics		Higuchi Kinetics		Korsmeyer–Peppas kinetics	
		R^2	K_0	R^2	K_1	R	K_H	R^2	*n*
F_1	pH 7.4	0.908	7.058	0.566	0.2303	0.987	29.234	0.651	0.973
F_2	pH 7.4	0.920	6.931	0.577	0.231	0.986	28.42	0.653	0.967
F_3	pH 7.4	0.534	6.828	0.976	0.233	0.7936	26.91	0.2236	0.977
F_4	pH 7.4	0.930	6.625	0.582	0.228	0.917	26.71	0.658	0.963
F_5	pH 7.4	0.920	6.931	0.577	0.231	0.986	28.42	0.653	0.967
F_6	pH 7.4	0.921	6.512	0.581	0.228	0.916	26.43	0.665	0.972
F_7	pH 7.4	0.926	6.423	0.595	0.234	0.9862	26.145	0.684	0.986
F_8	pH 7.4	0.920	6.931	0.577	0.231	0.986	28.42	0.653	0.967
F_9	pH 7.4	0.921	6.823	0.615	0.254	0.9872	26.345	0.674	0.976

Little swelling of IPN hydrogel had been noticed at low pH. Fig. 9 manifest pH effects on imbibition of IPN hydrogel

The concentration of LTZ which is released at specified time intervals had been measured spectrophotometrically. Release of drug was greater in the media with high pH due to more swelling of IPN hydrogels at higher pH. When the release behavior of drug from different formulations were contrived contrary to time, it was observed that drug release was increased by increasing the percentage of HPMC (F_4 to F_6) & PVP (F_1 to F_3).

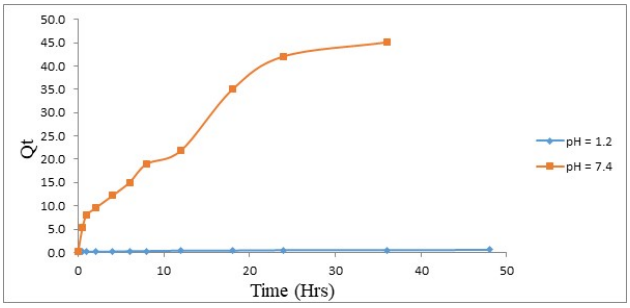

Fig. 8: Swelling index of hydrogels at pH-1.2 and pH-7.4

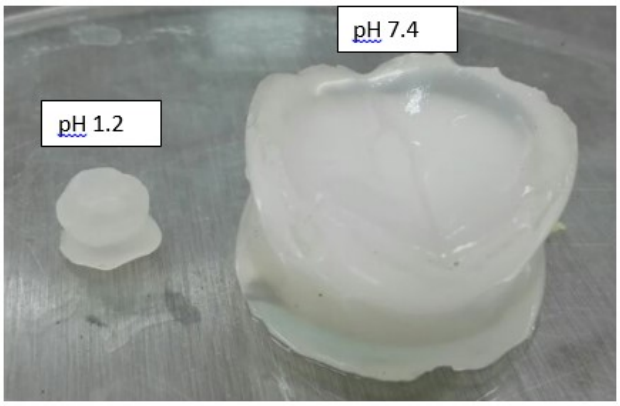

Fig. 9: Effect of different pH on MBA cross-linked MAA/HPMC/PVP IPN hydrogels

Kinetics of drug release

In order to get insight into release rate and mechanism of drug release from polymeric system, different kinetic models were applied to all samples where Higuchi model was best fitted mathematical model for all IPN hydrogels indicating towards diffusion controlled mechanism of drug release. (Mikolaszek *et al*., 2020). Higuchi model explains drug release from matrix systems where drug loading exceeds from drug solubility in matrixes (Choi *et al*., 2019), thus maximum portion of drug disperse as solid aggregates in polymeric matrix while small portion dissolves into matrix (Choi and Cha, 2019). Furthermore, this model is based on assumptions that amount of entrapped drug is greater than drug solubility in release media and drug diffuses outward at constant rate and release media maintains sink conditions (Quadrado and Fajardo, 2020). From table 2, it is observed that majority of formulations follow zero order kinetics for drug release.

Acute-Oral Toxicity Study

To conduct toxicity study F_6 IPN polymeric formulation was selected to given the maximum DEE as well as *in-vitro* cumulative LTZ release. A group had been kept as a control (C) group while group B had been kept as a treatment-group. Dose selected for administering is 5g/kg body-weight, none of the unwanted effects had been seen within the treatment group B as well as no mortality occurred along the 14-day period of acute oral toxicity study as same as the control group A. Histopathological study of various vital organs such as, heart, liver, stomach, lungs, spleen as well as the kidney of A and B group have been depicted in fig. 11.

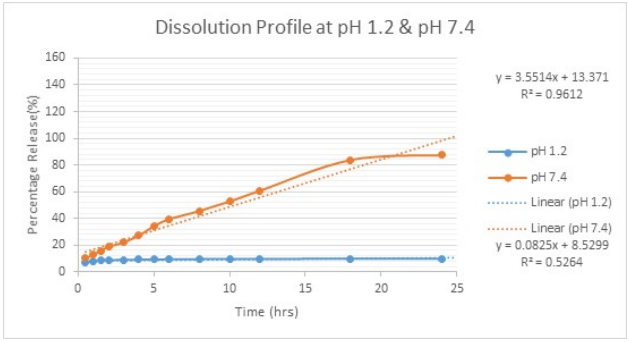

Fig. 10: Cumulative percent drug releases of hydrogels at pH 1.2 and pH 7.4

No significant variation exists within histopathological studies of group A and B when administered with IPN hydrogels none of the formulation-related toxic effects were observed in group B. The pericardium, myocardium, as well as the endocardium of B group had been in usual appearance while no hypertrophy occur within heart muscles. The mucosa lining the stomach was also usual to normal with none observed symptoms of ulceration.

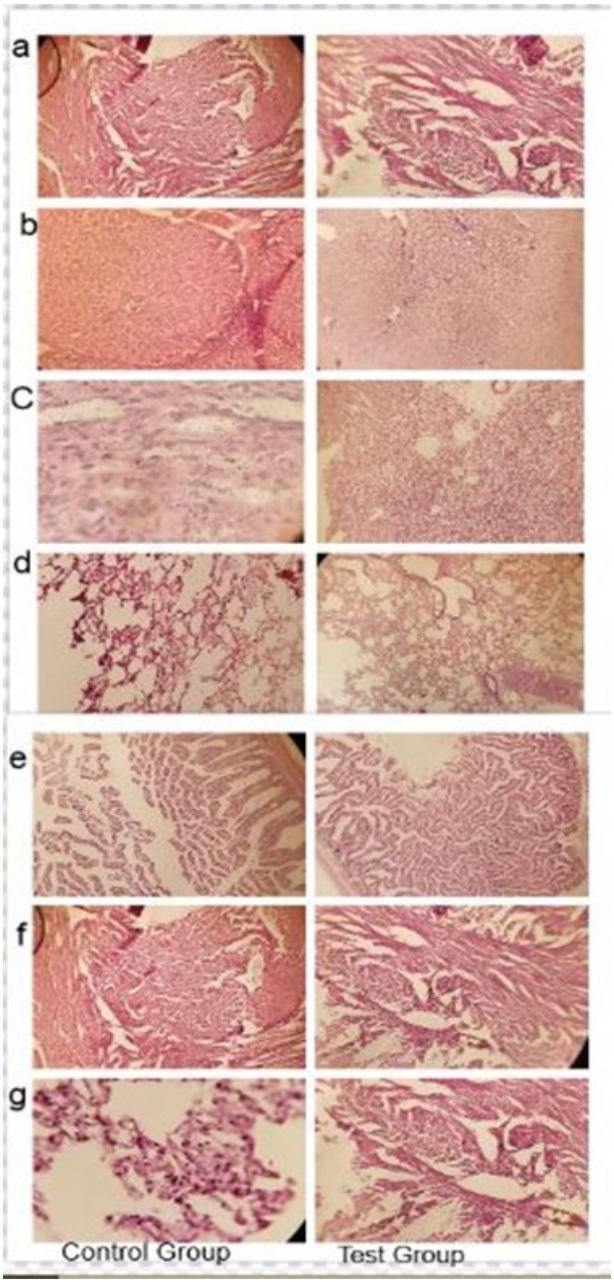

Fig. 11: Histological examination of various tissues (a) heart, (b) liver, (c) kidney, (d) spleen, (e) lungs, (f) intestines, (g) stomach of rabbits belonging to the control group I and test group II (treated by LTZ)

Lungs depicted no signs relating to the thickening of blood-vessels walls surrounding bronchus, while no bronchial or alveolar damage, represented typical physiology. Kidney also demonstrates usual morphological shape and size. Liver lobules belonging to B group were present along with clear dividing lines, as same as that of A group. Spleen sinus was utterly normal in both the groups, depicting no evidence of toxicity. To conclude, no gross difference in histopathological observation had been detected within the control and treatment groups. Therefore, a dose level of up to 5g/kg body weight of formulated IPN polymeric formulation had been tolerated for 14-day study length period, depicting that formulated IPN polymeric network are sufficiently non-toxic.

DISCUSSION

As the FTIR spectrum of HPMC dictates, the broad absorption band at 3456cm^{-1} suggests the stretching frequency of the -OH groups. The bands at 2932 and 1065cm^{-1} depict the stretching vibration of C-H as well as C-O bonds, respectively. On the other hand, the bending vibration of -OH groups on the HPMC is shown at 1381cm^{-1} (Wang *et al*., 2016). The PVP spectrum illustrates its signature in the form of CO (1660cm^{-1}) and C-N (1290cm^{-1}). The sharp peak at 1600cm^{-1} is indicating the aromatic stretching (C=C). Methylene bending (H-C-H) illustrates peak at 1496 that is small as well as 1457cm^{-1} (Zhu *et al*., 2010). MAA shows peaks at 1635cm^{-1} that indicate significant absorption due to carbonyl group, at 1697cm^{-1} due to vinyl groups peak was observed and due to -OH of R-COOH broad band ranging through 3000 - 3450cm^{-1} (Kumar *et al*., 2006). In IPN hydrogel FTIR, each small peaks at 1400cm^{-1}, 1247cm^{-1}, 1166–1056cm^{-1}, 756cm^{-1}, 693cm^{-1} as well as 510cm^{-1} have been allotted to OCH_2 wagging vibration, aromatic ether stretching, as well as asymmetric C-O-C stretching, C-H out of plane deformation vibration or ring deformation vibration and skeletal vibration. Other invariant peaks of methylene H-C-H bending at 1490 and 1450cm^{-1} have confirmed the polymerization of HPMC, PVP as well as MAA. The abridged intensity level of aromatic ether stretching at 1243cm^{-1} as well as aromatic ring deformation at 757 and 692cm^{-1} corroborated the abridged MAA monomer concentration. The information obtained through FTIR spectra of HPMC, PVP and MAA has been utilized to predict the formation mechanism of HPMC-co-poly (MAA)/PVP hydrogelpolymer as depicted in fig. 2.

Porous structure of IPN hydrogel is may be result of ionic and hydrophilic group in formulated interpenetrating polymeric formulation (Zhao *et al*., 2006). Hence, integrating the hydrophilic constituent within polymeric formulation has enhanced hydrophilicity as well as subsequent porosity of hydrogels (Zhang *et al*., 1999). Such porous architecture as well as connectivity of pores within formulated IPN hydrogel indicates towards its role in swelling and de-swelling kinetics.

It is known that cross linking restricts the molecular movements and increases the Tg. The Tg peak shift is small for low degree of cross linking but is large for high degree of cross linking [52]. Moreover, HPMC cross linking replaces the van der Waals interactions by covalent bonds (ester). Hence, the flow of heat is higher in the case of covalent bond interactions than weak force interactions. This further indicates that the formed hydrogel acts as a single network due to cross linking (Dharmalingam and Anandalakshmi, 2019).

In PXRD due to peak shifting, peaks intensity level was also sufficiently decreased, disclosing interaction within LTZ as well as IPN. This depicts that the conjugated as well as entangled LTZ are not able to make crystal lattice within polymer while they remain in an amorphous state. Such manifestations draw up a conclusion that drugs are distributed in the IPN that fulfills the requisite necessary requirement of a better drug delivery system (DDS) (Malik *et al*., 2020).

Gel% and yield % increases with MAA concentration as higher concentration of monomer provide more active sites for linkage (Rasib *et al*., 2018). Inverse relation of PVP concentration on yield% and gel time may possibly due to increasing viscosity with high PVP concentration which hinders in polymerization reaction (Bhattacharyya *et al*., 2013). HPMC concentration relation to yield% and gel time may be due to availability of free radicals with increasing concentration of polymer (Samanta and Ray, 2014).

HPMC effect on swelling of hydrogel is possibly due to ionization of sulfonate groups of APS at pH 7.4 as this pH value is higher than its pKa value. Ionized sulafonate groups creates strong repulsive forces which produce expansion of the polymeric network (Kim and Lee, 1992, El-Hag Ali, 2012). HPMC matrix form gel when in contact with water, due to methyl (hydrophobic – water-hating) and hydroxyl-propyl (hydrophilic – water-loving, more or less) substitutions, the meshwork of hydrogen bondings (H-bondings) present within cellulose are disrupted apart. The hydrophobic (water-hating) interactions present within methyl groups and water may result in self-aggregation of the HPMC chains. The aggregation is zipped up via interactions with water (also referred to as H-bonding), that results in the gelation of HPMC in nearly all cases. HPMC depicts a fairly sufficient affinity to water molecules, resulting in excessive water solubility of the polymer. The controverting effects of the hydrophobic (water-hating) methyl groups as well as hydrophilic (water-loving) hydroxyl-propyl groups produce HPMC the swelling ability within the aqueous media (Joshi, 2011). Effects of PVP on swelling phenomenon was primarily imputable to the oxygen atoms of the carbonyl group present in PVP that may form hydrogen bonds along with the H atoms present in water molecules, that endued PVP with sufficiently strong hydrophilicity (water-loving ability) to bond with sufficient amount of water (Huang *et al*., 2017). Little swelling at low pH may be due to strong cross linking between molecules of carboxylic group in MAA and hydroxyl group of HPMC with groups in MBA. Decreased swelling was observed in anionic groups having less repulsive force due to protonation of hydroxyl group at low pH (Mujumdar *et al*. (2007), Sadeghi and Yarahmadi, 2011).

CONCLUSION

IPN hydrogels were prepared successfully by free radical polymerization. Developed IPN hydrogels showed pH dependent swelling and release kinetics which is possibly due the chemical crosslinking intricated electrostatic interaction and hydrogen bonding. Among all samples, swelling behavior and drug entrapment efficiency of sample (F_6) of IPN hydrogel was high. IPN hydrogel water absorbency increases with increase in either monomer (MAA) or polymers (HPMC & PVP) concentration. . The percentage of drug release was also investigated from various kinetic models and found that formulation (F_6) followed the zero order kinetics for drug release and Higuchi model explained mechanism of drug release. FT-IR analysis confirmed the fusion of monomer (MAA) with polymers (HPMC & PVP). In this study, we have observed that how the unique pendant acidic and basic properties of HPMC, PVP and MAA offer for systemic delivery of LTZ at controlled rate by free radical polymerization.

ACKNOWLEDGMENTS

The authors acknowledge their thankful gratifications to Rahid Latif College of Pharmacy and Ameer & Adnan Pharmaceuticals, for providing lab support to conduct this research study investigation.

REFERENCES

Acharjya SK, Mallick P, Panda P, Kumar KR and Annapurna MM (2010). Spectrophotometric methods for the determination of letrozole in bulk and pharmaceutical dosage forms. *J. Adv. Pharm Technol. Res.,* **1**(3): 348.

Ahmadi F, Oveisi Z, Samani SM and Amoozgar Z (2015). Chitosan based hydrogels: Characteristics and pharmaceutical applications. *Res. Pharm. Sci.,* **10**(1): 1-18.

Ahmed EM (2015). Hydrogel: Preparation, Characterization and applications: A review. *JAR,* **6**: 105-121.

Akhtar MF, Hanif M and Ranjha NM (2016). Methods of synthesis of hydrogels a review. *SPJ.,* **24**(5): 554-559.

Anwar M, Pervaiz F, Shoukat H, Noreen S, Shabbir K, Majeed A and Ijaz S (2020). Formulation and evaluation of interpenetrating network of xanthan gum and polyvinylpyrrolidone as a hydrophilic matrix for

controlled drug delivery system. *Polymer Bulletin*, pp.1-22.

Anwar M, Pervaiz F, Shoukat H, Noreen S, Shabbir K, Majeed A and Ijaz S (2021). Formulation and evaluation of interpenetrating network of xanthan gum and polyvinylpyrrolidone as a hydrophilic matrix for controlled drug delivery system. *Polymer Bulletin,* **78**(2021): 59-80.

Barkat K, Ahmad M, Minhas MU and Khalid I (2017). Oxaliplatin-loaded crosslinked polymeric network of chondroitin sulfate-co-poly (methacrylic acid) for colorectal cancer: Its toxicological evaluation. *J. Appl. Polymer. Sci.,* **134**(38): 45312.

Bhattacharyya R, Ray SK and Mandal B (2013). A systematic method of synthesizing composite superabsorbent hydrogels from crosslink copolymer for removal of textile dyes from water. *JIEC,* **19**(4): 1191-1203.

Bhowmik D, Gopinath H, Kumar BP, Duraivel S and Kumar KS (2012). Controlled release drug delivery systems. *J. Pharm. Innov.,* **1**: 24-32

Chavda H and Patel C (2010). Chitosan superporous hydrogel composite-based floating drug delivery system: a newer formulation approach. *J. Pharm. Bioallied. Sci.,* **2**(2): 124.

Choi G and Cha HJ (2019). Recent advances in the development of nature-derived photocrosslinkable biomaterials for 3d printing in tissue engineering. *Biomater. Res.,* **23**(19): 18.

Choi SH, Cho IH and Park S (2019). Gemcitabine-incorporated polyurethane films for controlled release of an anticancer drug. *Biomater. Res.,* **23**(19): 1-7.

Dharmalingam K and Anandalakshmi R (2019). Fabrication, characterization and drug loading efficiency of citric acid crosslinked nacmc-hpmc hydrogel films for wound healing drug delivery applications. *Int. J. Biol. Macromol.,* **134**(2019): 815-829.

Dutta S, Samanta P and Dhara D (2016). Temperature, pH and redox responsive cellulose based hydrogels for protein delivery. *Int. J. Biol. Macromol,* **87**(2016): 92-100.

El-Hag Ali A (2012). Removal of heavy metals from model wastewater by using carboxymehyl cellulose/ 2-acrylamido-2-methyl propane sulfonic acid hydrogels. *J. Appl. Polym. Sci.,* **123**(2): 763-769.

Fu G and Soboyejo W (2010). Swelling and diffusion characteristics of modified poly (N-isopropylacryl-amide) hydrogels. *Mater. Sci. Eng., C* **30**(1): 8-13.

Ganji F and Vasheghani FE (2009). Hydrogels in controlled drug delivery systems.

Group BIGC (2005). A comparison of letrozole and tamoxifen in postmenopausal women with early breast cancer. *NEJM,* **26**(353): 2747-2757.

Huang M, Hou Y, Li Y, Wang D and Zhang L (2017). High performances of dual network pva hydrogel modified by PVP using borax as the structure-forming accelerator. *Designed Monomers and Polymers,* **20**(1): 505-513.

Joshi SC (2011). Sol-Gel behavior of hydroxypropyl methylcellulose (HPMC) in ionic media including drug release. *Materials,* **4**(10): 1861-1905.

Kamoun EA (2016). N-succinyl chitosan–dialdehyde starch hybrid hydrogels for biomedical applications. *J. Adv. Res.,* **7**(1): 69-77.

Kazemi S, Sarabi AA and Abdouss M (2016). Synthesis and characterization of magnetic molecularly imprinted polymer nanoparticles for controlled release of letrozole. *Korean J. Chem. Eng.,* **33**(2016): 3289-3297.

Khalid I, Ahmad M, Minhas MU and Barkat K (2018). Synthesis and evaluation of chondroitin sulfate based hydrogels of loxoprofen with adjustable properties as controlled release carriers. *Carbohydr. Polym.,* **181**(2018): 1169-1179.

Khan QJ, Reddy PS, Kimler BF, Sharma P, Baxa SE, O'dea AP, Klemp JR and Fabian CJ (2010). Effect of vitamin d supplementation on serum 25-hydroxy vitamin d levels, joint pain, and fatigue in women starting adjuvant letrozole treatment for breast cancer. *Breast Cancer Res Treat,* **119**(1): 111.

Khanum H, Ullah K, Murtaza G and Khan SA (2018). Fabrication and *in vitro* characterization of hpmc-g-poly (Amps) hydrogels loaded with loxoprofen sodium. *Int. J. Biol. Macromol.,* **120**(part B): 1624-1631.

Kim CJ and Lee PI (1992). Hydrophobic anionic gel beads for swelling-controlled drug delivery. *Pharm. Res.,* **9**(1): 195-199.

Kim SW, Bae YH and Okano T (1992). Hydrogels: Swelling, drug loading, and release. *Pharm. Res.,* **9**(1): 283-290.

Kumar A, Lahiri SS and Singh H (2006). Development of pegdma: Maa based hydrogel microparticles for oral insulin delivery. *Int.J.Pharm.,* **323**(1-2): 117-124.

Malik NS, Ahmad M and Minhas MU (2017). Cross-linked β-cyclodextrin and carboxymethyl cellulose hydrogels for controlled drug delivery of acyclovir. *Plos One,* **12**: 1-17

Malik NS, Ahmad M, Minhas MU, Tulain R, Barkat K, Khalid I and Khalid Q (2020). Chitosan/xanthan gum based hydrogels as potential carrier for an antiviral drug: fabrication, characterization and safety evaluation. *Front. Chem.,* **8**: 50.

Mikolaszek B, Kazlauske J, Larsson A and Sznitowska M (2020). Controlled drug release by the pore structure in polydimethylsiloxane transdermal patches. *Polymers,* **12**(7): 1520.

Mujumdar SK, Bhalla AS and Siegel RA (2007). Novel hydrogels for rhythmic pulsatile drug delivery. macromolecular symposia. Wiley Online Library, pp.338-344.

Quadrado RF and Fajardo AR (2020). Microparticles based on carboxymethyl starch/chitosan polyelectrolyte complex as vehicles for drug delivery systems. *Arab. J. Chem.,* **13**(1): 2183-2194.

Radwan R, Abdelkader A, Fathi HA, Elsabahy M, Fetih G and El-Badry M (2021). Development and evaluation of letrozole-loaded hyaluronic acid/chitosan-coated poly (d, l-lactide-co-glycolide) nanoparticles. *J. Pharm. Innov.*, pp.1-12.

Rasib S, Ahmad Z, Khan A, Akil H, Othman M, Hamid Z and Ullah F (2018). Synthesis and evaluation on ph- and temperature-responsive chitosan-p (maa-co-nipam) hydrogels. *Int. J. Biol. Macromol.,* **108**: 367-375.

Rusu AG, Popa MI, Lisa G and Vereştiuc L (2015). Thermal behavior of hydrophobically modified hydrogels using tga/ftir/ms analysis technique. *Thermochim. Acta,* **613**(2015): 28-40.

Sadeghi M and Yarahmadi M (2011). Synthesis and characterization of superabsorbent hydrogel based on chitosan-g-poly (acrylic acid-coacrylonitrile). *Afr. J. Biotechnol.,* **27**(2): 12265-12275.

Samanta HS and Ray SK (2014). Synthesis, characterization, swelling and drug release behavior of semi-interpenetrating network hydrogels of sodium alginate and polyacrylamide. *Carbohydr. Polym.,* **99**: 666-678.

Sami AJ, Khalid M, Jamil T, Aftab S, Mangat SA, Shakoori A and Iqbal S (2018). Formulation of novel chitosan guargum based hydrogels for sustained drug release of paracetamol. *Int. J. Biol. Macromol.,* **108**(2018): 324-332.

Saraf S (2010). Applications of novel drug delivery system for herbal formulations. *Fitoterapia,* **81**(7): 680-689.

Siddiqa AJ, Chaudhury K and Adhikari B (2014). Letrozole dispersed on poly (vinyl alcohol) anchored maleic anhydride grafted low density polyethylene: A controlled drug delivery system for treatment of breast cancer. *Colloids Surf B Biointerfaces,* **116**(2014): 169-175.

Singh B and Sharma V (2014). Influence of polymer network parameters of tragacanth gum-based pH responsive hydrogels on drug delivery. *Carbohydr. Polym.,* **101**(2014): 928-940.

Sohail M, Ahmad M, Minhas MU, Ali L, Khalid I and Rashid H (2015). Controlled delivery of valsartan by cross-linked polymeric matrices: Synthesis, *in vitro* and *in vivo* evaluation. *Int. J. Pharm.,* **487**(1-2): 110-119.

Soman A, Mathew F, Chacko A, Alias M and Poosan GV (2014). interpenetrating polymer network (ipn)-hydrogels. *J. Pharm. Innov.,* **3**(8, Part A): 59.

Varelas CG, Dixon DG and Steiner CA (1995). Zero-order release from biphasic polymer hydrogels. *J. Control. Release,* **34**(3): 185-192.

Wang T, Chen L, Shen T and Wu D (2016). Preparation and properties of a novel thermo-sensitive hydrogel based on chitosan/hydroxypropyl methylcellulose/ glycerol. *Int. J. Biol. Macromol.,* **93**(part A): 775-782.

Zhang Y, Won CY and Chu CC (1999). Synthesis and characterization of biodegradable network hydrogels having both hydrophobic and hydrophilic components with controlled swelling behavior. *J. Polym. Sci. A: Polym Chem,* **37**(24): 4554-4569.

Zhao Y, Kang J and Tan T (2006). Salt-, Ph-and temperature-responsive semi-interpenetrating polymer network hydrogel based on poly (aspartic acid) and poly (acrylic acid). *Polymer,* **47**(22): 7702-7710.

Zhu X, Lu P, Chen W and Dong J (2010). Studies of uv crosslinked poly (N-vinylpyrrolidone) hydrogels by ftir, raman and solid-state nmr spectroscopies. *Polymer,* **51**(14): 3054-3063.